



Human Paleontology and Prehistory

Stratigraphy and paleoenvironment during the Late Pliocene at Masol paleonto-archeological site (Siwalik Range, NW India): Preliminary results



Stratigraphie et paléoenvironnement du site paléonto-archéologique de Masol (chaîne des Siwaliks, Inde du Nord-Ouest) durant le Pliocène tardif : résultats préliminaires

Alina Tudryn^{a,*,b}, Salah Abdessadok^c, Julien Gargani^{a,b},
Anne Dambricourt Malassé^c, Claire Gaillard^c, Anne-Marie Moigne^d,
Cécile Chapon Sao^c, Mukesh Singh^e, Vipnesh Bhardwaj^e, Baldev Karir^e,
Serge Miska^{a,b}

^a Université Paris-Sud, Laboratoire GEOPS, UMR8148, Bâtiment 504, 91405 Orsay, France

^b CNRS, 91405 Orsay, France

^c Histoire naturelle de l'Homme préhistorique (HNHP, UMR 7194), Département de Préhistoire, Muséum national d'Histoire naturelle, Paris, France

^d Histoire naturelle de l'Homme préhistorique (HNHP, UMR 7194), Centre d'Études et de Recherches Préhistoriques (CERP), Tautavel, France

^e Society for Archaeological and Anthropological Research, Chandigarh, India

ARTICLE INFO

Article history:

Received 29 January 2015

Accepted after revision 5 May 2015

Available online 13 August 2015

Handled by Yves Coppens and Anne Dambricourt Malassé

Keywords:

Upper Siwalik

Pliocene

Chandigarh anticline

Masol paleonto-archeological site

Clay minerals

Subathu sub-basin

Paleoenvironment

Water divide

ABSTRACT

The Quranwala zone (Siwalik Range, NW India) is known for its Late Pliocene vertebrates. Since 2008, cut marks and stone tools have been collected from Masol. The sedimentary series belongs to the Subathu sub-basin. These sub-Himalayan deposits contain repetitive sequences (~170 m thick) of silt/clays and sandstones corresponding to the cyclical influx of detrital material in a fluvial environment. Particular features of lithological units allow identification of the stratigraphic position of different paleonto-archeological localities. A first pale environmental reconstruction was enabled by analysis of clay and magnetic minerals. Iron minerals such as haematite and goethite indicate dominant oxic conditions during and after deposition. Clay minerals are of detrital origin, and were supplied from Himalaya by rivers. Illite, the result of physical weathering, is dominant. Smectite present in the lower part of the sequence, was probably supplied from Lesser Himalaya (Suresh et al., 2004). Its presence suggests that the studied area was still a paleo-drainage area for major river(s) during the time considered here.

© 2015 Académie des sciences. Published by Elsevier Masson SAS. This is an open access article under the CC-BY-NC-ND license (<http://creativecommons.org/licenses/by-nc-nd/4.0/>).

* Corresponding author.

E-mail address: alina.tudryn@u-psud.fr (A. Tudryn).

R É S U M É

Mots clés :

Upper Siwalik
Pliocène
Anticlinale de Chandigarh
Site paléonto-archéologique de Masol
Minéraux argileux
Sous-bassin de Subathu
Paléoenvironnement
Ligne de partage des eaux

La zone de Quranwala (Pliocène final, chaîne frontale des Siwaliks, Inde) est connue pour ses Vertébrés fossiles. Depuis 2008, des traces de boucherie et des outils lithiques ont été récoltés à Masol. La série sédimentaire s'inscrit dans le sous-bassin de Subathu. Ces dépôts sous-himalayens renferment une série de séquences répétitives (~170 m d'épaisseur) de silt/argile et de sable/grès. Des caractéristiques lithologiques identifient les localités paléonto-archéologiques et leur position stratigraphique. Une reconstitution paléoenvironnementale préliminaire a été faite grâce à des analyses d'argiles et de minéraux magnétiques. Les minéraux de fer – hématite et goethite – indiquent des conditions oxygènes dominantes pendant et après le dépôt. Les argiles sont d'origine détritique, elles ont été transportées par les rivières depuis l'Himalaya. L'illite, résultat d'une altération physique, est dominante. La smectite présente dans la partie inférieure de la séquence provient du bas Himalaya (Suresh et al., 2004). Sa présence correspondrait alors à un paléodrainage de rivière(s) majeure(s) avant l'instauration d'une ligne de partage des eaux entre deux bassins (Indus et Gange actuels).

© 2015 Académie des sciences. Publié par Elsevier Masson SAS. Cet article est publié en Open Access sous licence CC-BY-NC-ND (<http://creativecommons.org/licenses/by-nc-nd/4.0/>).

1. Introduction

The Siwalik Range, also known as the Siwalik Hills, or Siwalik Frontal Range (SFR) in Asian prehistory studies, is the southernmost and geologically youngest WNW-ESE range of the Himalayan chain. This sub-Himalayan zone was extensively studied for sedimentology, tectonics, paleoenvironment, fauna, paleoclimate, stratigraphy, etc. (e.g. Barnes et al., 2011; Burbank et al., 2012; Delcaillau et al., 2006; Kumar et al., 2003, 2007; Nanda, 2002; Pilgrim, 1913; Ranga Rao, 1993; Sanyal et al., 2010; Singh and Tandon, 2010; Thomas et al., 2002; Tripathi, 1986). The Siwalik Frontal Range is a result of the folding and uplift of the Siwalik Group, which is a sequence of continental sediments deposited in the Himalayan Siwalik-Ganga-Indus foreland basin from Middle Miocene to Middle Pleistocene (Fig. 1a). The Indian plate's northward push resulted in the Himalayan foreland basin uplift, which started in Middle/Late Pleistocene (Barnes et al., 2011). The combined action of tectonics and monsoons resulted in intense erosion and exhumation of sediment rich in fossils of aquatic and terrestrial vertebrata from the Masol anticline, NW of India (Fig. 1b, Fig. 2a). Sediments of this anticline, which is also known as the Chandigarh anticline (Barnes et al., 2011), are well known from the literature (e.g. Barnes et al., 2011; Nanda, 2002; Ranga Rao, 1993). Its older part outcrops in the core of the anticline and contains a faunal assemblage belonging to the Tatrot, and more precisely to the so-called Quranwala Zone (or Quaranwala Zone), which represents the Late Pliocene, whereas younger sediments belong to the Pleistocene and represent Pinjor (or Pinjaur) faunal assemblage (Ranga Rao, 1993).

Since 2008, the Siwaliks Indo-French Programme of Research has been conducted in the Masol anticline area by the Indian Society for Archaeological and Anthropological Research of Chandigarh and the French Prehistorical Mission in India from the National Museum of Natural History, Paris (Dambricourt Malassé, 2016). Numerous fossils, including bovid bones with intentional cut marks and stone tools, have been collected in the core of this anti-

cline (Abdessadok et al., 2016; Chapon Sao et al., 2016a; Dambricourt Malassé et al., 2016a, 2016b; Gaillard et al., 2016; Moigne et al., 2016) (Fig. 1). The discovery of bones with intentional cut marks in such a stratigraphic context is compatible with the recent dating of the Early Pleistocene human settlement in China (Longgupo cave, 2,48 Ma) (Han et al., 2015) and with predictions concerning human settlements in the Upper Indus Basin since Late Pliocene (Dennell, 2010), giving support to the 'Out of Africa 1' scenario before 1.8 Ma (Coppens, 2016).

Fossils were collected in several separated, so-called Masol paleonto-archeological localities numbered from Masol 1 to Masol 13 (Fig. 2b). These localities form slopes and platforms in actual landscape eroded by the Patiali Rao stream and its tributaries, such as the Pichhli choe. Fossils have been found either in situ or as redeposited. Masol 1, 2 and 3 are located to the north of the Masol village, Masol 4, 5 and 6 extend to the northwest, and localities from Masol 7 to Masol 13 extend to the southeast of the village. The Late Pliocene age of the fossiliferous sediments has been confirmed by a magnetostratigraphic study realized at the Masol 1 locality (Chapon Sao et al., 2016b). These Late Pliocene sediments are composed of silts/clays and sandstones cyclically deposited in the fluvial environment and different layers are very similar in profile. Moreover, the Middle and Late Quaternary post-depositional processes related to active tectonics (folding and faulting), erosion, redeposition (colluviums, fluvial terraces) resulted in an important modification of the initial position of the sediment (see also Gargani et al., 2016). This situation complicates the correlation between different Masol paleonto-archeological localities and the identification of their exact stratigraphic position.

In this paper, we present the results of investigations conducted during fieldworks in spring 2014 and 2015 and the results of laboratory analyses of samples collected in 2014. The aim of this work was (1) the establishment of the complete lithological log for Late Pliocene sediments available in the Masol anticline, (2) the identification of the sediment sequences with particular features to allow

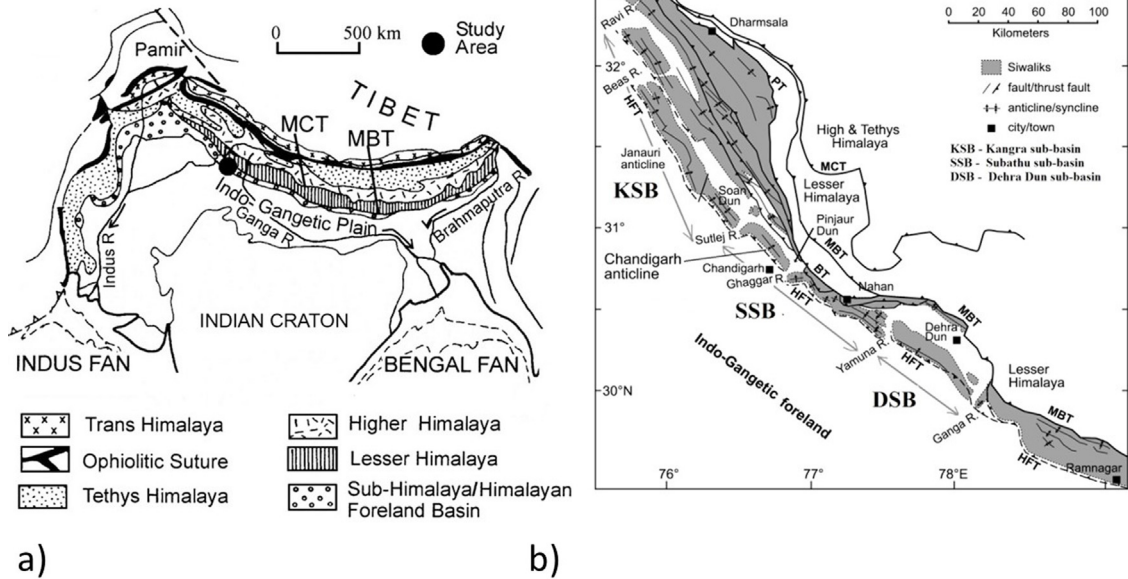


Fig. 1. a) Simplified geologic map of the Himalayan range including the Siwalik Himalayan Foreland Basin, Indian craton and the surrounding area, after Kumar et al. (2003); b) simplified geologic map of a part of the Himalayan Foreland Basin, the Kangra, Subathu and Dehra Dun sub-basins, after Barnes et al. (2011). MCT: Main Central Thrust; MBT: Main Boundary Thrust; HFT: Himalayan Frontal Thrust; BT: Bilaspur Thrust; PT: Palampur Thrust; R: river. **Fig. 1.** Carte géologique simplifiée : a) chaîne Himalayenne, y compris le bassin d'avant-pays des Siwaliks himalayens, le Craton indien et la région environnante d'après Kumar et al. (2003) ; b) une partie du bassin d'avant-pays des Siwaliks himalayens, les sous-bassins de Kangra, de Subathu et de Dehra Dun, d'après Barnes et al. (2011). MCT : « Main Central Thrust » ; MBT : « Main Boundary Thrust » ; HFT : « Himalayan Frontal Thrust » ; BT : « Bilaspur Thrust » ; PT : « Palampur Thrust » ; R : rivière.

their recognition in different Masol paleonto-archeological localities (Masol 1, Masol 2 to Masol 13), and (3) the stratigraphic correlation of the fossiliferous layers from different Masol localities. Additionally, the analysis of granulometry and carbonate contents, as well as identification of clay and magnetic minerals, was performed in order to establish some mineralogical characteristics of the sequence. These characteristics allow studies of the environmental evolution of the area, and the first results of these analyses are presented here.

2. Upper Siwalik subgroup – background

The SFR (Siwalik Frontal Range) is about 2,400 km long area that starts almost from the Indus and ends close to the Brahmaputra, and its width varies from 10 to 50 km. The SFR is a result of the folding and uplift of the sediment from Siwalik Group, which started from Middle/Late Pleistocene due to Indian plate push northward (for more details see Gargani et al., 2016). The Siwalik Group is a thick sequence of continental sediments deposited in the Himalayan Siwalik-Ganga-Indus foreland basin from Middle Miocene to Middle Pleistocene. In its northwestern part, the more than 5000 m thick Siwalik sequence consists of sandstone, claystone and conglomerate alternations, with coarsening upwards, reflecting the progressive uplift of the Himalaya from which they are derived (Ranga Rao, 1993). On the basis of rich assemblages of terrestrial vertebrate faunas, the youngest, the Upper Siwalik subgroup, known in India mainly from the Jammu and Chandigarh regions, is subdivided into Tatrot and Pinjor (Pilgrim, 1913) (Fig. 2c).

The limit between these two formations is marked by the change in magnetic polarity between Gauss and Matuyama chronos (2.58 Ma), the Plio/Quaternary limit (Ranga Rao, 1993; Ranga Rao et al., 1995; for a summary see Chapon Sao et al., 2016b).

On the basis of lithologic criteria, the ONGC (Oil Natural Gas Commission) identified for the Upper Siwalik subgroup in Jammu region: (1) Parmandal Sandstone, (2) the Nagrota Formation (pink siltstone-claystone alternations with subordinate earthy sandrock), and (3) the youngest, Boulder Conglomerate (Ranga Rao, 1993). The Boulder Conglomerate is devoid of fossils, and started between 1.2 and 0.6 Ma at different sites (Fig. 2c). In the Chandigarh region, close to the Masol paleonto-archeological localities, ONGC evidenced Upper Siwalik in the Patiali Rao stream section as Masol Formation (alternation of sandstone and claystone) and four conglomeratic units, Rupar I, II, III, IV (Fig. 2c). On faunal evidence, the Masol Formation was correlated with Tatrot, Rupar I, II, III with Pinjor faunal zones, and the conglomerates of Rupar IV with the Boulder Conglomerate which started here at ~0.6 Ma. A 50 m thick section towards the top of the Tatrot Formation, called the Quranwala Zone, is characterized by rich vertebrate fossils corresponding to the Plio/Pleistocene faunal transition. This is unlike the situation in other localities (Nagrota and Parmandal) where the characteristic taxa of Tatrot such as *Hipparion* are replaced rather abruptly by younger Pinjor fauna like *Equus*, *Cervus* and *Archidiskodon* (Ranga Rao, 1993; for more details see Moigne et al., 2016). After Nanda (2002), two biostratigraphic interval zones, *Elephas planifrons* (3.6–2.6 Ma) and *Equus sivalensis* (2.6 to 0.6 Ma) are recognised here.

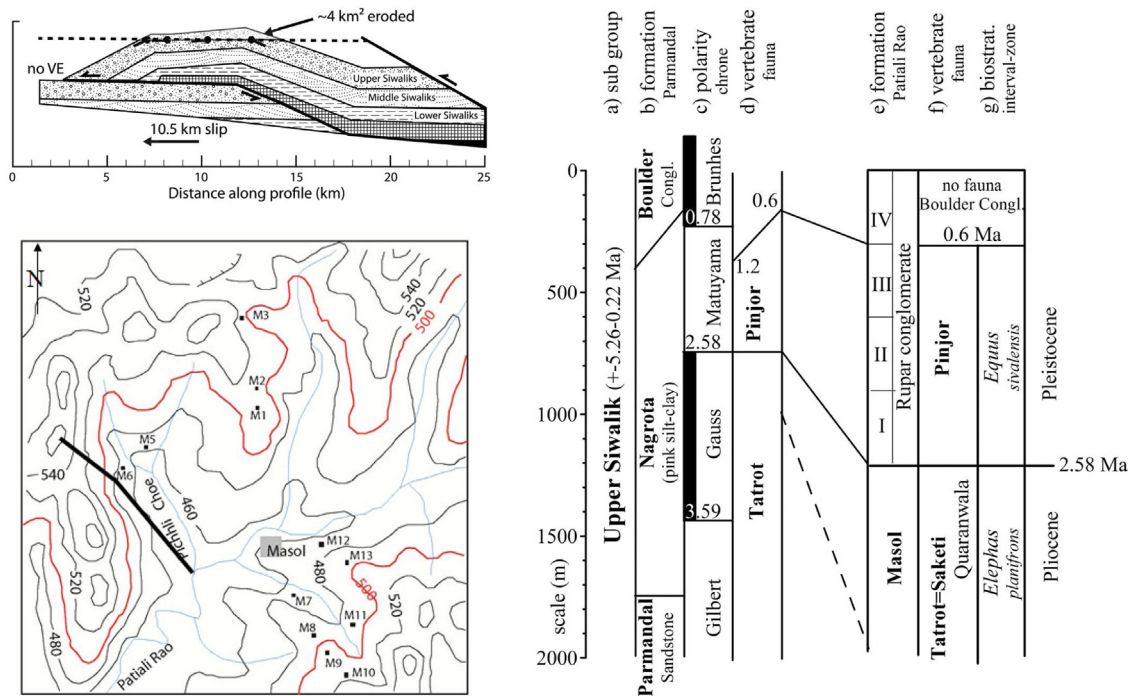


Fig. 2. (Color online.) Top left: The Chandigarh anticline, after Barnes et al. (2011); for more details, see Gargani et al. (2016). Bottom left: topographic map of the Masol village environments; grey square – Masol village, small black squares marked M1, M2, ... M13 denote different paleonto-archaeological localities and the black line shows the section of the lithological log presented in Fig. 5. Right: simplified stratigraphy of the Upper Siwalik subgroup, northwestern part of the Siwalik Range: a) Upper Siwalik subgroup; b) lithological units for Upper Siwalik subgroup distinguished by ONGC (Oil Natural Gas Commission) in northwest Siwalik (Jammu region, ~340 km NW from Chandigarh); the sequence is 2500 m thick in Parmandal (Parmandal Formation), and the last unit, the Boulder Conglomerate is diachronic; c) magnetostratigraphy: black – normal polarity chron, white – inverse polarity chron, for more details see Chapon Sao et al., 2016b, this issue; d) vertebrate faunas assemblages after Pilgrim (1913) in Ranga Rao (1993); e) lithological units after ONGC close to the Masol village near Chandigarh (Masol Formation); f) vertebrate fauna assemblage in the Masol Formation which defines the Quranwala Zone; g) biostratigraphic interval zones in the Masol Formation. Numbers indicate ages in Ma. Synthesis after Ranga Rao (1993), Nanda (2002) and authors discussed in these papers.

Fig. 2. (Couleur en ligne.) En haut à gauche : l'anticlinal de Chandigarh d'après Barnes et al. (2011) ; pour plus de détails, voir Gargani et al. (2016). En bas à gauche : carte topographique des environs du village de Masol ; carré gris – village de Masol, petits carrés noirs – localités paléonto-archéologiques depuis Masol 1 jusqu'à Masol 13, la ligne noire indique la section où a été réalisée la coupe lithologique présentée sur la Fig. 5. À droite : stratigraphie simplifiée de l' « Upper Siwalik subgroup », au nord-ouest de la chaîne des Siwalik : a) « Upper Siwalik subgroup » ; b) unités lithologiques distinguées par l'ONGC au nord-ouest des Siwaliks (région du Jammu, ~340 km au nord-ouest de Chandigarh) ; pour plus de détails, voir le texte ; c) magnétostratigraphie : noir – période de polarité normale, blanc – période de polarité inverse ; pour plus de détails, voir Chapon Sao et al. (2016b) ; d) assemblages de faunes de vertébrés d'après Pilgrim (1913) in Ranga Rao (1993) ; e) unités lithologiques d'après ONGC proches du village de Masol près de Chandigarh (formation Masol) ; f) assemblages de faunes vertébrées dans la formation Masol, qui définit la zone Quranwala ; g) zones d'intervalle biostratigraphique dans la formation Masol. Les chiffres indiquent les âges en Ma. Synthèse d'après Ranga Rao (1993), Nanda (2002) et les auteurs cités dans ces études.

3. Material and methods

3.1. Principles

Granulometric evidence indicates the dynamics of transport of and/or distance from the detrital material sources during deposition. Clay minerals deposited in the fluvial environment reflect the intensity of chemical and physical weathering of their source area (Chamley, 1989). This weathering depends on the lithology, climate and morphology of the environment under consideration and results in the formation of superficial soils and sediments. In temperate and warm humid and semi-arid climates, chemical weathering prevails, and kaolinite or smectite appear. Under weakly hydrolytic conditions in dry climates, physical weathering prevails, and illite and chlorite often appear, since the production of clays depends essentially on increased direct rock erosion. The abundance of

illite can also indicate strong erosion related to tectonically rejuvenated relief or to deforestation and not necessarily to weak hydrolytic climatic conditions. Post-depositional processes can also modify detrital clay minerals.

Magnetic parameters allow estimation of the ferromagnetic minerals present in the sediment. The presence of these minerals (e.g. iron oxides: magnetite Fe_3O_4 , maghemite $\gamma\text{Fe}_2\text{O}_3$, haematite $\alpha\text{Fe}_2\text{O}_3$, oxyhydroxides: goethite FeOOH and sulphides: greigite Fe_3S_4) depends on the source area, and conditions during deposition and after, where early diagenetic processes can modify the detrital fraction, and new minerals can appear. Low field magnetic susceptibility (χ) depends on the ferromagnetic minerals (which can carry remanent magnetisation) present in sediment, if their content is very low, then χ depends on the paramagnetic and/or diamagnetic minerals which cannot carry remanent magnetisation. The magnetic hysteresis parameters: coercivity (B_c), remanent coercivity

(Bcr), saturation magnetisation (Ms) and remanent magnetisation (Mrs), allow discrimination between different ferromagnetic materials. The thermomagnetic behaviour of the sediment allows identification of ferromagnetic minerals through their Curie temperature, the temperature at which they are demagnetised. Some of these minerals are unstable on heating, but can still be identified because of their specific thermomagnetic behavior (maghemite, goethite). This is the basis of environmental magnetism as defined by Thompson and Oldfield (1986) and it is used by many authors.

3.2. Fieldwork and laboratory analyses

During fieldwork in spring 2014 and 2015, a stratigraphic framework based on lithological studies was designed, and magnetic susceptibility measurements and sampling for laboratory analysis performed in the area of the Masol village where the Masol Formation is most complete. This was possible in the western part of the Pichhli choe stream, starting from its confluence with the principal stream Patiali Rao and proceeding until the top of the sequence passing through the Masol 6 paleonto-archaeological locality (black line in Fig. 2b and Fig. 3a).

The low field magnetic susceptibility was measured during the fieldwork directly on each identified lithological unit (after cleaning to obtain fresh surface) with a Bartington MS-2 susceptibility meter. Samples were collected near to the places where magnetic susceptibility was measured, and then analysed in the laboratories of National Museum of Natural History and GEOPS-University Paris-Sud (GEOPS-UPS) for magnetic and clay minerals, Ca and Mg carbonate content and grain size. Particle size analyses of samples were performed by laser granulometry on fractions of sediment under to 2 mm with a Malvern Mastersizer 2000 instrument. Carbonate contents were measured by titration with bromophenol blue solution. X-ray diffraction (XRD) on oriented mounts of non-calcareous clay-sized (<2 µm) particles was used to identify clay minerals with a PANalytical diffractometer, following the laboratory routine of the GEOPS-UPS (Liu et al., 2004, 2008). Three XRD runs were conducted following air-drying, ethylene-glycol solvation for 24 h, and heating at 490 °C for 2 h. Identification of clay minerals was based on the position of the (001) series of basal reflections on the three XRD diagrams. Semi-quantitative estimates of peak areas of the basal reflections for the main clay mineral groups of smectite (including mixed layers) (15 to 17 Å), illite (10 Å) and kaolinite/chlorite (7 Å) were carried out on the glycolated curve (Holtzapffel, 1985) with MacDiff software (Petschick, 2000). Relative proportions of kaolinite and chlorite were determined based on the ratio 3.57/3.54 Å of the peak areas. Evaluation of each clay mineral had an accuracy of 5%. In order to identify magnetic minerals in sediment, the thermomagnetic behavior and magnetic hysteresis of several bulk sediment samples were measured. The thermomagnetic behavior was obtained by using a horizontal force translation balance in an air atmosphere and a magnetic field of 0.375 T. Magnetic hysteresis measurements were made on discrete samples (5 mg to 15 mg of

dry, bulk sediment) with an alternating gradient magnetometer (AGM 2900 – Micromag) at the LSCE – CNRS/CEA laboratory at Gif-sur-Yvette, France. A peak-applied field of 1 T was used for hysteresis measurements and the results were corrected for the paramagnetic and diamagnetic contribution of the matrix minerals. After removal of this contribution, saturation magnetisation (Ms), saturation remanent magnetisation (Mrs) and coercive force (Bc) were obtained from the hysteresis loop. Remanent coercivity (Bcr) was obtained through step-wise application of backfields to remove the saturation remanent magnetisation.

4. Results

4.1. Lithological description

The studied Late Pliocene sequence contains cyclically deposited layers of sands (sandstones now) and finer grain-sized sediments – silts/clays (Fig. 3b). Layers of sandstones are more or less homogeneous; their thickness varies from several tenths of centimeters to several meters. They are rich in quartz and in white mica and therefore in their fresh state they are grey; nevertheless, in the outcrops, some of them stay grey, but others are yellow or rose-colored. They are not strongly consolidated, they become hard when they are dry and in humid conditions, they disintegrate into sand. Sometimes, they contain oblique stratification, nodules or other consolidated forms. Especially in the upper part of the sequence, these layers of sandstones/sand contain levels with gravel and pebbles, and are even locally replaced by conglomerate (Fig. 3c). Gravel and pebbles are heterogeneous in size, nature (including quartzitic) and degree of rounding. Generally, the sandstones/sand are quite well resistant to weathering and erosion. They form cliffs and are interlaid by often thinner layers of finer silty to clayish sediments, which are evidently eroded more easily and often form platforms between cliffs (Fig. 3a). These silty/clayish sediments are mostly brownish (rarely grey) and sometimes colored (yellow, orange, reddish) because of the oxydo-reduction of iron (e.g. c6 in Fig. 3a).

The sequence contains a series of 17 pairs of layers defined during the fieldwork as silty/clayish and sandstone/sandy units (Fig. 5a). The adopted numbering starts at the bottom (c1-s1, c2-s2 . . .), i.e. at the junction of Patiali Rao and Pichhli choe (Fig. 2b), “c” meaning silty/clayish and “s” sandstone/sandy units. Thicknesses are approximate because of lateral variation. The 17 silty/clayish and sandstone/sandy pairs counted represent the first order of the lithological changes. In these layers, the second order of lithological changes is often observed, and fine silty levels can appear locally in sandstone/sandy units and sandy levels can also be present in silty/clayish units (Fig. 3b and Fig. 3d).

A more detailed lithological description of the sediment is not the focus of this work, with the exception of unit c6, which is thicker than other silty/clayish units and is ~20 m thick. We distinguished four sub-units: (1) c6-1, a clear brown silty sequence containing locally one or two sandy levels (Fig. 3d); (2) c6-2, very characteristic and well

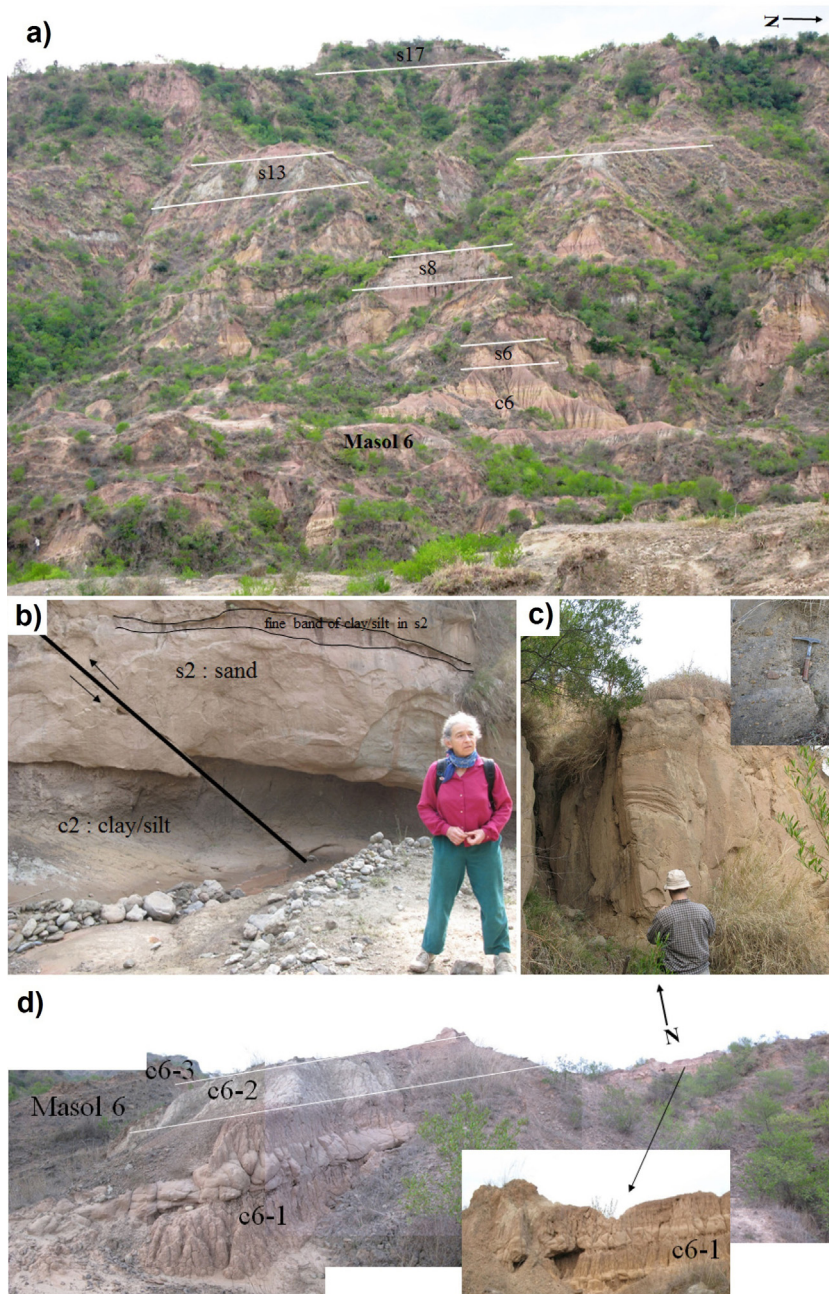


Fig. 3. (Color online.) Photographs of sediments exhumed from Chandigarh anticline close to Masol village: a) western part of the site above Masol 6 paleonto-archeological locality where lithological units are marked (for explanation see the text); b) silty/clayish c2 and sandstone/sandy s2 units; c) sandstone/sandy unit s15, and conglomerate in unit s16; d) part of unit c6: sub-unit c6-1 with laterally changing sandy banks.

Fig. 3. (Couleur en ligne.) Photographies de sédiments de l'anticlinal de Chandigarh à proximité du village de Masol : a) partie ouest du site, au-dessus de la localité Masol 6, les différentes unités lithologiques sont indiquées (pour explication, voir le texte). Détails des différentes unités : b) unités argilo-sableuse c2 et grés-sableuse s2 ; c) unité grés-sableuse s15 et conglomérat dans l'unité s16 ; d) partie de l'unité c6 : détails de la sous-unité c6-1 avec les changements latéraux des bancs de sable.

observable in the landscape, a grey/white silty layer, ~1 m thick (Fig. 3d and Fig. 4a), and in the upper part of this sub-unit a ~10 cm thick level is present, which enhances the stratification; (3) c6-3, brownish-reddish silt with traces of the first step of the lateritisation and some concretions enriched in the iron minerals found here (Fig. 4a), contains,

as in sub-unit c6-2, ~10 cm thick levels which enhance the stratification; and finally (4) c6-4, more than 10 m thick, which is formed by several silty and sometimes sandy fine levels, each one differentiated by yellowish, reddish, orange, brownish colors which follow the stratification (c6 in Fig. 3a and c6-4 in Fig. 4a).

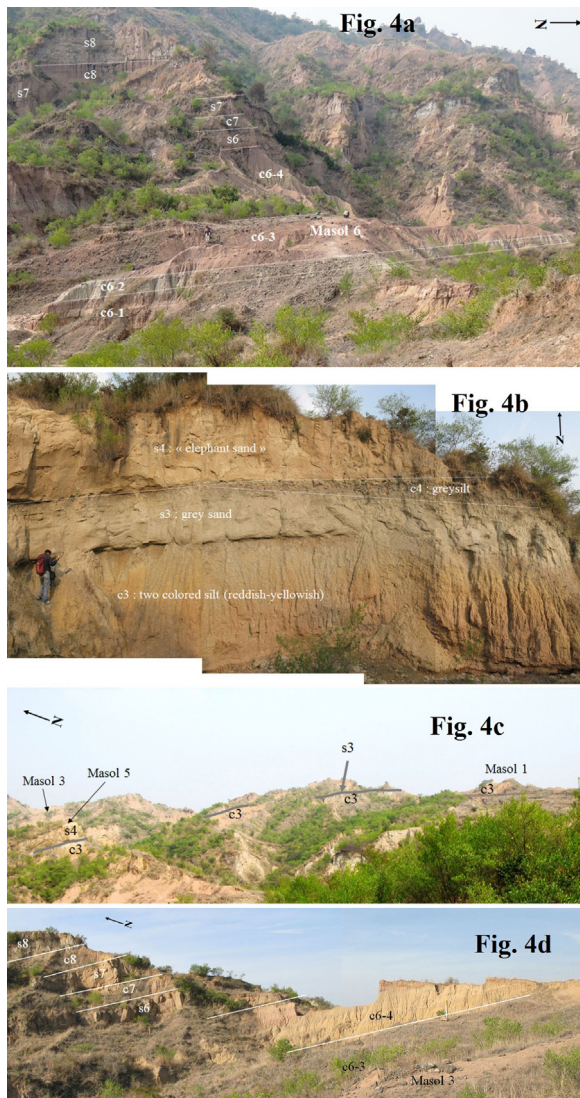


Fig. 4. (Color online.) Photographs of sediments exhumed from Chandigarh anticline close to Masol village: (a) Masol 6 paleonto-archeological locality and lithological units from c6 to s8, including characteristic sequence of sub-units from c6-1 to c6-4; (b) characteristic sequence of c3-s3-s4; (c) Masol 1, 3 and 5 localities: their stratigraphic position and corresponding lithological units; (d) Masol 3 locality: its stratigraphic position and corresponding lithological units.

Fig. 4. (Couleur en ligne.) Photographies de sédiments de l'anticlinal de Chandigarh à proximité du village de Masol : (a) localité Masol 6 et unités lithologiques de c6 jusqu'à s8, y compris une séquence caractéristique des sous-unités de c6-1 à c6-4 ; (b) séquence caractéristique de c3-s3-s4 ; (c) localités Masol 1, 3 et 5 et leur position stratigraphique d'après les corrélations des unités lithologiques ; (d) localité Masol 3 et sa position stratigraphique, d'après les corrélations des unités lithologiques.

4.2. Granulometry, carbonate contents, clay and magnetic minerals

Samples for granulometry and analysis of clay minerals and carbonate contents were collected in 2014 and 2015 close to the layers where the magnetic susceptibility measurements were taken directly in outcrops. The samples of 2014 have been analysed.

Granulometry performed on particles with a diameter under 2 mm reflects mostly changes between sandstones and silty/clayish units identified during the fieldwork (Fig. 5a). Proportions of clays and silts as well as main grain sizes are presented in Fig. 5c and Fig. 5d. The considered grain sizes present higher and more scattered values in the lower part of the sequence than in the upper one.

Ca and Mg carbonate content varies between 10% and 50% (Fig. 5e); it is slight in the lower part of the sequence, increases, but changes between units c5 and c6 (45 m to 70 m), and becomes higher above.

Among clay minerals, illite is dominant, and its content is frequently as high as ~60% (Fig. 5f). Nevertheless, in the lower part of the sequence until unit c6-2 it is lower and it even became below 10% in unit s3 and in one point above, in unit c11. When illite content is low, smectite presents higher values, and becomes dominant at 80% for units s3 and c11. Variations in the illite and smectite contents are independent of the grain size of the rock. Chlorite and kaolinite present values lower than 20% all along the sequence (Fig. 6a).

Low field magnetic susceptibility presents low values throughout the studied sequence, indicating low content of magnetic minerals in the sediment as a whole. Nevertheless, there is clear difference between sandstone units "s", with lower magnetic susceptibility, and finer grain size units "c", where magnetic susceptibility is higher (Fig. 5b). This relation is systematic, and although sometimes its value is low in the thin level of unit "c", it indicates that the level is rich in sand, as confirmed by laser granulometry measurements. Clearly higher values of magnetic susceptibility were obtained for concretions found in sub-unit c6-3 (these concretions are hereafter called Fe-rich concretions), which represents the early step of lateritisation, and in unit c16.

Magnetic hysteresis and Curie balance experiments were performed for Fe-rich concretions and for samples from units c2, s3 and c6-2. Results for units c2, s3 and c6-2 are similar. Magnetic hysteresis loops, as well as hysteresis characterising parameters (Bc, Bcr, Mrs/Ms) for samples c2 and Fe-rich concretions, are presented in Fig. 6b and Fig. 6c. Both samples present hysteresis loops, which are constricted in the middle section, and wider above and below the middle section; in sample c2 (Fig. 6b) the constriction is more pronounced. Such "wasp-waisted" hysteresis loops in geological materials indicate the coexistence of at least two different magnetic components with contrasting coercive fields (e.g. Day et al., 1977; Roberts et al., 1995; Tauxe et al., 1996; Wasilewski, 1973). In such conditions, the coercive field (Bc) is largely controlled by "soft", low-coercivity components such as ferrimagnetic magnetite or maghemite, whereas the coercivity of remanence (Bcr) is controlled by "hard", high-coercivity components such as canted antiferromagnetic haematite or goethite. The degree of the constriction in the middle section of the magnetic loop depends on the relative contribution of each component. Wasp-waisted hysteresis loops may reflect (1) a mixture of different grain sizes of a single magnetic mineral, (2) a mixture of different magnetic materials with largely different coercivities, or (3) a combination of both (Roberts et al., 1995). In the presence of "soft", high magnetic

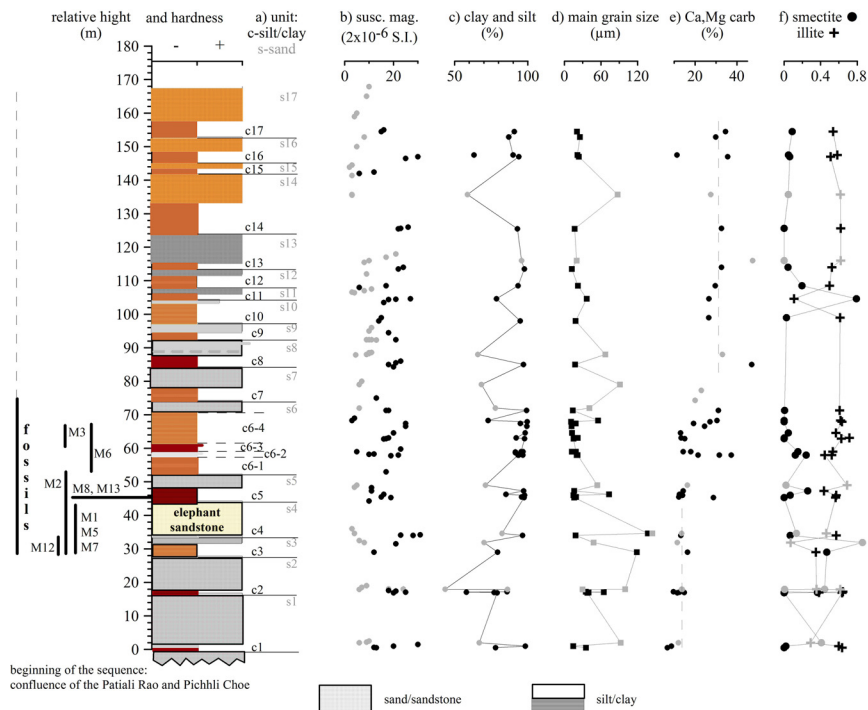


Fig. 5. (Color online.) Sedimentary sequence from Masol/Chandigarh anticline with simplified lithology and relative hardness of sediments, as well as: a) different silty/clayish “c” and sandstone/sandy “s” units; b) magnetic susceptibility; c) contents of fraction under 63 μm (sum of clay and silt); d) mean grain size of particles; e) Ca and Mg carbonate content; f) smectite and illite contents. Grey color of a), b), c), d), e) and f) symbols indicates measurements made on sandstone/sandy “s” units, black color indicates measurements made in silty/clayish “c” units. On the left of the log, are marked areas rich in fossils (solid line) and poor in fossils (dashed line) in the sequence and the stratigraphic position of different Masol paleonto-archeological localities.

Fig. 5. (Couleur en ligne.) Séquence sédimentaire de l’anticlinal de Masol/Chandigarh, avec la lithologie simplifiée et la dureté relative des sédiments, ainsi que : a) unités argilo-silteuses « c » et grés-sableuses « s » ; b) susceptibilité magnétique ; c) teneurs de la fraction inférieure à 63 μm , d) taille moyenne des particules ; e) teneurs en carbonate de Mg et de Ca ; f) teneurs en smectite et en illite. La couleur grise des symboles en a), b), c), d), e) et f) indique des mesures effectuées sur des niveaux des unités grés-sableuses « s » ; la couleur noire indique des mesures effectuées sur des niveaux des unités argilo-silteuses « c ». Sur la gauche du log, les couches riches en fossiles (ligne continue), pauvres en fossiles (ligne discontinue) et la position stratigraphique des différentes localités paléonto-archéologiques de Masol sont indiquées.

moment minerals (magnetite or maghemite), “hard” minerals with weak magnetic moments (haematite, goethite) must be abundant to cause wasp-waisted magnetic loops. The hysteresis loop form, low B_c and high B_{cr} for Fe-rich concretions from sub-unit c6-3 (Fig. 6c), indicate the mixture of the “soft” mineral(s) such as magnetite and/or maghemite and “hard” mineral(s) such as haematite and/or goethite. The hysteresis loop form and B_c and B_{cr} values in sample c2 indicate the dominance of high-coercivity minerals such as goethite and haematite.

The thermomagnetic behavior of samples from unit c2 shows the mixture of a mineral, which undergoes demagnetisation before 200 $^{\circ}\text{C}$ and haematite, with Curie temperature of 680 $^{\circ}\text{C}$ (Fig. 6d). The decrease of the magnetisation until ~ 200 $^{\circ}\text{C}$ is probably owed to the presence of an iron oxyhydroxide, goethite, which loses water in such temperatures, and is transformed into haematite (e.g. Tarling, 1983). The concretion from sub-unit c6-3 shows also a small decrease of magnetisation until 200 $^{\circ}\text{C}$ (Fig. 6e). The second total demagnetisation, which occurs at 400 $^{\circ}\text{C}$, and the irreversible cooling curve suggest the presence of maghemite (e.g. Tarling, 1983; Thompson and Oldfield, 1986). This is consistent with magnetic hysteresis results; the use of these methods allows identification of

the goethite and haematite in samples from unit c2 and goethite and maghemite in the Fe-rich concretion from sub-unit c6-3.

5. Discussion

5.1. Characteristic lithological units and stratigraphic position of different Masol paleonto-archeological localities

The series obtained for the sediment passing through the Masol 6 paleonto-archeological locality contains a repetitive sequence corresponding to a cyclical pattern of influx of detrital material in fluvial environmental conditions. This lithology and geomorphological features of the Masol anticline make it difficult to establish the precise stratigraphy and correlations between different Masol paleonto-archeological localities. Nevertheless, some layers present specific characteristics, which are easily identifiable. Unit c1, the sequence of units c3, s3 and s4, unit c6, and unit s13 are such examples.

At the beginning of the investigated sequence, unit c1, which is about 1.8 m thick, is formed by lower brownish and upper grey silt/clay, and is only one such situation

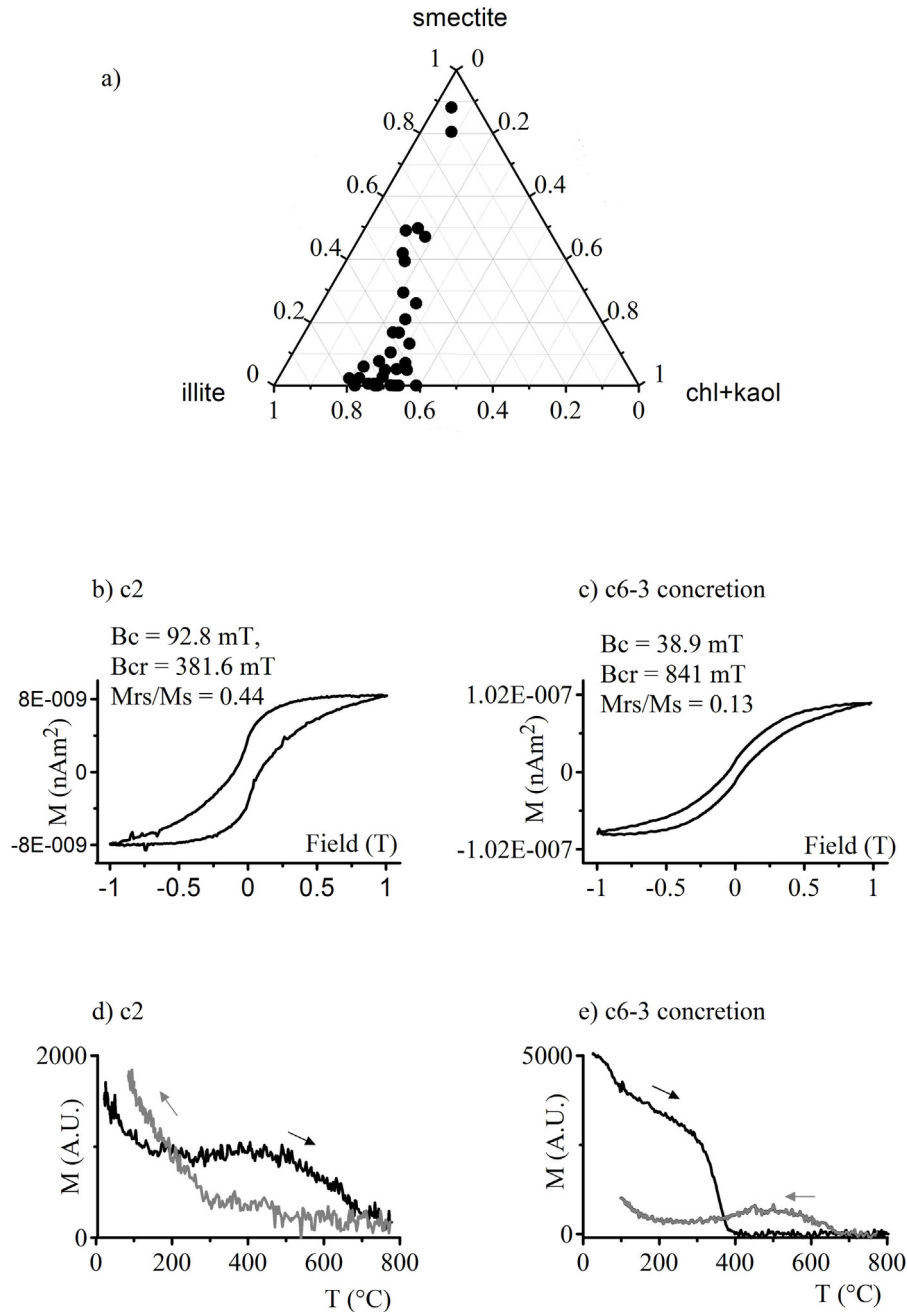


Fig. 6. Sedimentary sequence from Masol anticline: a) ternary diagram of illite, chlorite+kaolinite and smectite contents; magnetic hysteresis loop for sample from; b) unit c2; c) Fe-rich concretion from sub-unit c6-3; d) thermomagnetic curve for sample from unit c2; e) Fe-rich concretion from sub-unit c6-3.

Fig. 6. Séquence sédimentaire de l'anticlinal de Masol : a) diagramme ternaire des teneurs en : illite, chlorite + kaolinite et smectite. Cycle de l'hystérésis magnétique pour : b) échantillon de l'unité c2 ; c) concrétion riche en fer de la sous-unité c6-3 ; d) courbe thermomagnétique de l'échantillon de l'unité c2 ; e) concrétion riche en fer de la sous-unité c6-3.

observed. The sequence of units c3, s3 and s4 presents a unique change multicolored silt c3 several meters thick, clear grey sandstones/sand s3 ~1 m thick and usually, without thin c4, immediately above, sandstone s4, which is some meters thick. The c3 silt starts with a brownish colored sub-layer which is followed by grey, reddish and finally orange ones. The sandstone s4 has a clear rose

color on the surface and is underlined by lying below the clear/grey sandstone unit s3. The sandstone s4 is called elephant sandstone, because of the fossilized head of an elephant found *in situ* in its upper part (Fig. 4b). Unit c6 presents a thick sequence (~20 m) composed of 4 different and characteristic sub-units, c6-1, c6-2, c6-3 and c6-4, as described above. The particularity of this set is enhanced

by the presence of the fine grey/white c6-2 and thick multi-colored c6-4 sub-units (Fig. 4a). Unit s13 constitutes thick, clear grey sandstone rich in white mica, and it is composed of second order layers including fine-grained silty layers. Unit s13 is clearly visible in the landscape as an important cliff (Fig. 3a) above the Masol 6 paleonto-archeological locality and is present only in this part of the site and to the southeast of Masol village.

In the section obtained for lithological log, Masol 6 paleonto-archeological locality occupies unit c6 (Fig. 5). The lithological characteristics of the sedimentary sequence allowed the identification of the stratigraphic position for other Masol paleonto-archeological localities. Fig. 4a, Fig. 4c and Fig. 4d illustrate Masol 6, Masol 1, Masol 5 and Masol 3 and Fig. 5 summarizes the identifications, which were made. All identified Masol paleonto-archeological localities are positioned between units c3 and c6. High fossil contents were found from unit c3 to unit c7; above unit c7, they became scarce. Most of the fossils between c3 and c7 were redeposited and some of them come from upper layers. Nevertheless, numerous fossils are well preserved (for more details, see Moigne et al., 2016), and were collected on the slopes of the layer from which they were exhumed by erosion. That and the presence of fossils which were found *in situ* (e.g. in units c3, s4 and c6; for more details see Chapon Sao et al., 2016a) highlight recent and local redeposition, which is the result of a very young erosion. Such erosion related to high exhumation rate was also pointed out by Gargani et al. (2016).

5.2. Magnetic and non-magnetic parameters: preliminary results of the environmental reconstructions

The Himalayan Foreland Basin (HFB) characterized by the fluvial deposits, Siwalik molasse, is subdivided into several sub-basins, including Subathu (our study area is in its western part), Kangra to the northwest of Subathu, and to the east Dehra Dun (Fig. 1b). These sub-basins were extensively studied in particular for magnetostratigraphy, the evolution of the fluvial system during Pliocene and the Quaternary, the origin of these fluvial deposits and their nature, including clay and magnetic minerals (Kumar et al., 2003; Kumaravel et al., 2005, 2010; Ranga Rao, 1993; Ranjan and Banerjee, 2009; Sangode and Bloemendal, 2004; Suresh et al., 2004).

Kumar et al. (1999, cited in Suresh et al., 2004) documented transverse trunk drainage flowing southwest between 5.5 Ma and 1.77 Ma, and piedmont drainage flowing southeast between 4.8 Ma and 0.5 Ma. The first was attributed to the major rivers draining through Higher and Lesser Himalaya, while the piedmont drainage, tributaries of major rivers, drained through the Sub-Himalayan region. Interweaving of different sandy channel deposits was evident, but nevertheless the floodplain deposits of the two types of drainage were difficult to distinguish.

Our results show the changing sequence of finer and coarser grain-sized deposits, which reflects this fluvial environment. Magnetic susceptibility increases in silty sediments and decreases in sandy sediments. On the whole, there are lower contents of carbonate in the lower part of

the sequence, where smectite is also present, and higher main grain sizes were measured in the fraction of the sediment below 2 mm. In the upper part of the sequence, illite is clearly dominant, carbonate content is higher and increased contents of gravel and pebbles can be observed. The middle part of the sequence, which constitutes the Masol 6 paleonto-archeological locality, represents the transitional zone between the two parts of the sequence. A more detailed study of some levels from Masol 6, as well as from Masol 1 and Masol 13 paleonto-archeological localities, is presented in Abdessadok et al. (2016) and in Chapon Sao et al. (2016a).

The magnetic susceptibility obtained for all the studied sequence indicates on the whole rather low contents of magnetic particles. Nevertheless, the distribution of the magnetic particles changes between sandy and silty granulometric fractions, with clearly higher contents in the finer sediment units “c” and lower contents in the sandy sediment from units “s”. Preliminary results of the mineralogical identifications were obtained only to samples from four units from the lower part of the sequence. They show that goethite and haematite are dominant magnetic minerals. Moreover, they show that these two minerals are present in both granulometric – sandstone/sandy and silty/clayish sedimentary units and their presence indicates that oxic conditions dominated during deposition and after. The reddish, yellowish, orange and brown colors of sediment in different parts of the sequence indicate that other more or less amorphous forms of iron oxyhydroxides are present, too. The composition of magnetic minerals was obtained for soils and parent rocks (sandstones, siltstones and mudstones) in previous studies on the Late Pliocene part of the Upper Siwalik sequence in Subathu sub-basin (Kumaravel et al., 2010; Sangode and Bloemendal, 2004; Sangode et al., 2007). These results showed that haematite and goethite are dominant, with increased magnetic susceptibility in soil horizons, which are on the whole weakly developed, and lower magnetic susceptibility in parent rocks. Our study shows that the content of magnetic minerals varies even through silty/clayish and sandstone/sandy rocks, which can become parent rocks for soil development. In our study, c6-3 sub-unit shows early step of the lateritisation. The Fe-rich concretions from this sub-unit are composed of goethite and maghemite. The presence of the maghemite suggests locally reducing conditions during or after concretion formation. Further studies will allow accurate identification of the magnetic minerals in the whole sequence.

Chaudhri and Gill (1983), Rainverman and Suresh (1997) and Rainverman (2002) investigated Dehra Dun and the Kangra and western Subathu sub-basin's Siwalik sediments for clay minerals. They found abundant illite and smectite with wide zigzag pattern in Kangra and Dehra Dun but in the Subathu sub-basin they found no smectite. They suggested that smectite was supplied by major rivers, and documented two independent paleo-drainage systems, similar to the present-day Indus and Ganga systems (see also Clift and Blusztajn, 2005), separated by a water divide along the Subathu sub-basin. They suggested that the systems did not cross each other and that this water divide is an ancient feature. However, the study by

Suresh et al. (2004) shows high proportions of smectite in the eastern part of the Subathu sub-basin. Indeed, Suresh et al. (2004) identified grey sand/sandstone in the Upper Siwalik sequence as deposited by trunk drainage, and sands that they named “buff ribbon sandstone bodies” as deposited by piedmont drainage. They found changing but high contents of smectite in grey sandstones; in buff ribbon sandstones, illite was largely dominant. Contents of illite and smectite in mudstone depend on tributaries or major rivers flooding. The distribution of clay minerals observed in our study (western part of the Subathu sub-basin), and presented in Fig. 5f and in Fig. 6a, is very close to that obtained by Suresh et al. (2004), including the presence of the smectite.

Rainverman and Suresh (1997) and Rainverman (2002) observed higher contents of illite in the older part of the studied sequence, and smectite in the younger one. They suggested that illite could be of diagenetic origin. Nevertheless, Suresh et al. (2004) did not confirm this distribution and identified illite as being of detrital origin, the same result as that for higher contents of illite in the upper part of the sequence, which we obtained in this study. As detrital illite in sediments is caused by physical weathering, and is usually very abundant in high-relief regions (Chamley, 1989), Suresh et al. (2004) suggested Higher Himalaya was its source area in the studied region.

Smectite is a result of the chemical weathering of volcanic rocks and of other rocks in warm, contrasting wet/dry climates (Chamley, 1989). Rainverman and Suresh (1997) suggested that smectite in the studied sub-basins is a result of the weathering of volcanic rocks in the Lesser Himalaya; nevertheless, sediments rich in smectite studied by Suresh et al. (2004) contain only rare volcanic rocks. Another possible source of the smectite could be pedogenesis in situ; nevertheless, some mudstones studied by Suresh et al. (2004) are rich in smectite but do not have traces of pedogenesis. Therefore, Suresh et al. (2004) suggested that smectite formed in the Lesser Himalaya from volcanic and other rocks in the favorable climate and supplied the studied sub-basins. This is also suggested by our results, since we found very high contents of smectite in the sandy unit s3.

Our results and those obtained by Suresh et al. (2004) indicate the presence of smectite in the Subathu sub-basin, contrary to the previous studies, and the smectite here is of detrital origin. Therefore, it had to be supplied from its source area by a major river system, as indicated by Rainverman and Suresh (1997) and Rainverman (2002) for the Dehra Dun and Kangra sub-basins. Since the supply of smectite was attributed to major river activity, it indicates that the Subathu sub-basin was still paleo-drainage area for major river(s) during the Late Pliocene considered in our study before definitive water division.

The smectite in the Lesser Himalaya and Siwalik is of major importance for studies on the sediments from the Indus and Ganga/Brahmaputra deltas. Indeed, in paleoclimate reconstructions, sources of different clay minerals have to be well recognized. In sediments from the Bay of Bengal for instance, smectite can reflect changes in its sources (Deccan plateau or Himalaya) or changes in the weathering conditions (Derry and France-Lanord, 1997, cited in Suresh et al., 2004).

6. Conclusion

During the fieldwork in spring 2014 and 2015, we established a lithological log for the exhumed Late Pliocene sedimentary sequence, which was rich in fossils in the Masol (Chandigarh) anticline. Particular features of some lithological units allowed their recognition in different Masol paleo-archeological localities, and the identification of the stratigraphic position of these localities was made. These localities are concentrated in the narrow band between the so-called units c3 and c6.

Some fossils were found in situ, others were redeposited, and our results indicate that the redeposition is recent and local. Consequently, bovid bones with intentional cut marks found among numerous fossils in this stratigraphic position are older than 2.58 Ma, Pliocene/Pleistocene limit.

The contents of magnetic particles are quite low on the whole, but systematically higher in silty/clayish sediment and lower in sandstones/sand. Independently of the granulometric fraction, the canted antiferromagnetic minerals haematite and goethite are dominant. In the Fe-rich concretions from a unit with early soil formation maghemite is also present. The obtained results complement previous studies of magnetic minerals done on soils and parent rocks (without their differentiation) from the Upper Siwalik Subathu sub-basin (Kumaravel et al., 2010).

The distribution of clay minerals observed in this study, shows the dominant contribution of illite on the whole. Smectite, which is absent from the upper part of the sequence except at one point, is present and even dominant in some levels of the lower part of the sequence. This result shows that smectite is not only present in the Late Pliocene sediment from the eastern part of the Subathu sub-basin (Suresh et al., 2004) but is also evident in its western part.

Our results, like these obtained by Suresh et al. (2004), suggest that clay minerals in the studied sequence are principally of detrital origin, and were thus supplied here by rivers. Detrital illite in sediments is caused by physical weathering, and is usually very abundant in the Himalayan high-relief region as a whole. Suresh et al. (2004) suggested Higher Himalaya as the principal source area for illite, and they identified Lesser Himalaya as a source area for smectite as a result of the chemical weathering of various rocks in a warm, contrasting wet/dry climate.

Some authors (Chaudhri and Gill, 1983; Rainverman, 2002; Rainverman and Suresh, 1997) postulated two independent paleo-drainage systems for Late Pliocene, similar to the present day Indus and Ganga systems and separated by a water divide along the Subathu sub-basin. Our results and those obtained by Suresh et al. (2004) show the presence of detrital smectite in the Subathu sub-basin, the origin of which is the Lesser Himalaya. Smectite had to be supplied from its source area by a major river system, and suggests that the Subathu sub-basin was still paleo-drainage area for major river(s) during the Late Pliocene time considered in our study, before the establishment of a definitive water divide.

The presence of smectite in the Lesser Himalaya and Siwalik is of major importance for paleoclimate

reconstructions based on studies of the sediments from the Indus and Ganga/Brahmaputra deltas.

Acknowledgements

The Indo-French program of research “Siwaliks” is under the patronage of Professor Yves Coppens, College of France and Academy of Sciences, Institute of France, since 2012. It has been supported by the French Ministry of Foreign Affairs during three years (2012, 2013, 2014), by the National Museum of Natural History, Paris (Department of Earth Sciences in 2011, and Department of Prehistory in 2007, 2010 and 2011). We are grateful to the Archaeological Survey of India for explorations and excavation permits, the Department of Cultural Affairs, Archaeology and Museums of the Punjab Government and the Embassy of India in Paris for their administrative support and the French Embassy, New Delhi. We are grateful to the Sarpanch of Masol village, for his hospitality. The authors thank Luce Delabesse and Rémy Pichon for technical help and Piotr Tucholka for discussions. Maxence Descheemaeker and Thibault Josselin, Master and Licence students participated in this work.

References

- Abdessadok, S., Chapon Sao, C., Tudryn, A., Dambricourt Malassé, A., Gaillard, C., Singh, M., Karir, B., Moigne, A.M., Gargani, J., Bhardwaj, V., Pal, S., 2016. Sedimentological study of major paleo-archaeological localities of the Late Pliocene Quranwala Zone, Siwalik Frontal Range, northwestern India, in *Human origins on the Indian sub-continent*. C. R. Palevol 15, this issue.
- Barnes, J.B., Densmore, A.L., Mukul, M., Sinha, R., Jain, V., Tandon, S.K., 2011. Interplay between faulting and base level in the development of Himalayan frontal fold topography. *J. Geophys. Res.* 116, F03012, <http://dx.doi.org/10.1029/2010JF001841>.
- Burbank, D.W., Bookhagen, B., Gabet, E.J., Putko, J., 2012. Modern climate and erosion in the Himalaya. *C.R. Geoscience* 344, 610–626.
- Chamley, H., 1989. *Clay sedimentology*. Springer, New York, 623 p.
- Chapon Sao, C., Abdessadok, S., Tudryn, A., Dambricourt Malassé, A., Singh, M., Karir, B., Gaillard, C., Moigne, A.M., Gargani, J., Bhardwaj, V., 2016a. Lithostratigraphy of Masol paleo-archaeological localities in the Quranwala Zone, 2.6 Ma, northwestern India. In *Human origins on the Indian sub-continent*. C. R. Palevol 15, this issue.
- Chapon Sao, C., Abdessadok, S., Dambricourt Malassé, A., Singh, M., Karir, B., Bhardwaj, V., Pal, S., Gaillard, C., Moigne, A.M., Gargani, J., Tudryn, A., 2016b. Magnetic polarity of Masol 1 Locality deposits, Siwalik Frontal Range, Northwestern India. In *Human origins on the Indian sub-continent*. C. R. Palevol 15, this issue.
- Chaudhri, R.S., Gill, G.T.S., 1983. Clay mineralogy of the Siwalik Group of Simla Hills, northwestern Himalaya. *J. Geol. Soc. India* 24, 159–165.
- Clift, P.D., Blusztajn, J., 2005. Reorganization of the western Himalayan river system after five million years ago. *Nature* 438 (15), 1001–1003.
- Coppens, Y., 2016. Human origins on the Indian sub-continent. C. R. Palevol 15, this issue.
- Dambricourt Malassé, A., 2016. The first Indo-French Prehistorical Mission in Siwaliks and the discovery of anthropic activities at 2.6 million years. In *Human origins on the Indian sub-continent*. C. R. Palevol 15, this issue.
- Dambricourt Malassé, A., Singh, M., Karir, B., Gaillard, C., Bhardwaj, V., Moigne, A.-M., Abdessadok, S., Chapon Sao, C., Gargani, J., Tudryn, A., Calligaro, T., Kaur, A., Pal, S., Hazarika, M., 2016a. Anthropic activities in the fossiliferous Quranwala Zone, 2.6 Ma, Siwaliks of Northwestern India, historical context of the discovery and scientific investigations. In *Human origins on the Indian sub-continent*. C. R. Palevol 15, this issue.
- Dambricourt Malassé, A., Moigne, A.M., Singh, M., Calligaro, T., Karir, B., Gaillard, C., Kaur, A., Bhardwaj, V., Pal, S., Abdessadok, S., Chapon Sao, C., Gargani, J., Tudryn, A., Garcia Sanz, M., 2016b. Intentional cutmarks on bovid from the Quranwala Zone, 2.6 Ma Siwalik Frontal Range, NW India. In *Human origins on the Indian sub-continent*. C. R. Palevol 15, this issue.
- Day, R., Fuller, M.D., Schmidt, V.A., 1977. Magnetic hysteresis properties of synthetic titanomagnetites. *Phys. Earth Planet. Inter.* 13, 260–266.
- Delcaillau, B., Carozza, J.-M., Laville, E., 2006. Recent fold growth and drainage development: the Janauri and Chandigarh anticlines in the Siwalik foothills, northwest India. *Geomorphology* 76, 241–256.
- Dennell, R., 2010. Out of Africa I: current problems and future prospects, chap 15. In: Fleagle, J.G., Shea, J.J., Grine, F.E., Baden, A.L., Leakey, R.E. (Eds.), *Out of Africa I: the First Hominin Colonization of Eurasia*. pp. 247–273.
- Gaillard, C., Singh, M., Dambricourt Malassé, A., Bhardwaj, V., Karir, B., Kaur, S., Pal, S., Moigne, A.M., Sao Chapon, C., Abdessadok, S., Gargani, J., Tudryn, A., 2016. The lithic industries on the fossiliferous outcrops of the Late Pliocene Masol Formation, Siwalik Frontal Range, northwestern India (Punjab). In *Human origins on the Indian sub-continent*. C. R. Palevol 15, this issue.
- Gargani, J., Abdessadok, S., Tudryn, A., Chapon Sao, C., Dambricourt Malassé, A., Gaillard, C., Moigne, A.M., Singh, M., Bhardwaj, V., Karir, B., 2016. Geology and geomorphology of Masol paleo-archaeological site, Late Pliocene, Chandigarh anticline, Siwalik Frontal Range, NW India. In *Human origins on the Indian sub-continent*. C. R. Palevol 15, this issue.
- Han, F., Bahain, J.-J., Deng, C., Boëda, E., Hou, Y., Wei, G., Huang, W., Garcia, T., Shao, Q., He, C., Falguères, C., Voinchet, P., Yin, G., 2015. The earliest evidence of hominid settlement in China: combined electron spin resonance and uranium series (ESR/U-series) dating of mammalian fossil teeth from Longgupo cave. *Quatern. Int.*, <http://dx.doi.org/10.1016/j.quaint.2015.02.025>, in press.
- Holtzapfel, T., 1985. Les minéraux argileux : préparation, analyse, diffractométrie et détermination. *Soc. Geol. Nord Publ.* 12, 136.
- Kumar, R., Ghosh, S.K., Mazari, R.K., Sangode, S.J., 2003. Tectonic impact on the fluvial deposits of Plio-Pleistocene Himalayan foreland basin. *Sediment. Geol.* 158, 209–234.
- Kumar, R., Suresh, N., Sangode, S.J., Kumaravel, V., 2007. Evolution of the Quaternary alluvial fan system in the Himalayan foreland basin: Implications for tectonic and climatic decoupling. *Quatern. Int.* 159, 6–20.
- Kumaravel, V., Sangode, S.J., Kumar, R., Siddaiah, N.S., 2005. Magnetic polarity stratigraphy of Plio-Pleistocene Pinjor Formation (type locality), Siwalik Group, NW Himalaya, India. *Curr. Sci.* 88 (9), 1453–1461.
- Kumaravel, V.S.J., Siddaiah, N.S., Kumar, R., 2010. Interrelation of magnetic susceptibility, soil color and elemental mobility in the Pliocene-Pleistocene Siwalik paleosol sequences of the NW Himalaya, India. *Geoderma* 154, 267–280.
- Liu, Z., Colin, C., Trentesaux, A., Blamart, D., Bassinot, F., Siani, G., Sicre, M.A., 2004. Erosional history of the eastern Tibetan Plateau over past 190 kyr: clay mineralogical investigations from the southwestern South China Sea. *Marine Geol.* 209, 1–18.
- Liu, Z., Tuo, S., Colin, C., Liu, J.T., Huang, C.Y., Selvaraj, K., Chen, C.T.A., Zhao, Y., Siringan, F.P., Boulay, S., Chen, Z., 2008. Detrital fine-grained sediment contribution from Taiwan to the northern South China Sea and its relation to regional ocean circulation. *Marine Geol.* 255, 149–155.
- Moigne, A.M., Dambricourt Malassé, A., Singh, M., Bhardwaj, V., Gaillard, C., Kaur, S., Karir, B., Pal, S., Abdessadok, S., Chapon Sao, C., Gargani, J., Tudryn, A., 2016. The faunal assemblage of the paleo-archaeological localities of Masol Formation, Late Pliocene Quranwala Zone, NW India. In *Human origins on the Indian sub-continent*. C. R. Palevol 15, this issue.
- Nanda, A.C., 2002. Upper Siwalik mammalian faunas of India and associated events. *J. Asian Sci.* 21, 47–58.
- Petschick, R., 2000. MacDiff 4.2.3, unpublished computer program. Johann-Wolfgang Goethe Universität, Frankfurt, Cited 01-12-2001 <http://servermac.geologie.uni-frankfurt.de/Reiner.html>.
- Pilgrim, G.E., 1913. The correlation of the Siwaliks with mammal horizons of Europe. *Rec. Geol. Surv. India* 43 (4), 264–326.
- Rainverman, V., 2002. Foreland sedimentation in Himalayan Tectonic Regime – a relook at the orogenic process. Bishen Singh Mahendra Pal Singh, Dehra Dun, India, 375 p.
- Rainverman, V., Suresh, N., 1997. Clay mineral distribution in the Cenozoic sequence of the western Himalayan Foothills. *J. Indian Assoc. Sediment.* 16, 63–75.
- Ranga Rao, A., 1993. Magnetic-polarity stratigraphy of Upper Siwalik of north-western Himalayan foothills. *Curr. Sci.* 64 (11–12), 863–873.
- Ranga Rao, A., Nanda, A.C., Sharma, U.N., Bhalla, M.S., 1995. Magnetic polarity stratigraphy of the Pinjor Formation (Upper Siwalik) near Pinjore, Haryana. *Curr. Sci.* 68 (12), 1231–1236.
- Ranjan, N., Banerjee, D.M., 2009. Central Himalayan crystallines as the primary source for the sandstone-mudstone suites of the Siwalik Group: New geochemical evidence. *Gondwana Res.* 16, 687–696.

- Roberts, A.P., Cui, Y., Verosub, K.L., 1995. Wasp-waisted hysteresis loops: mineral magnetic characteristics and discrimination of components in mixed magnetic systems. *J. Geophys. Res.* 100 (B9), 909–917, 17, 924.
- Sangode, S.J., Bloemendal, J., 2004. Pedogenic transformation of magnetic minerals in Pliocene–Pleistocene palaeosols of the Siwalik Group, NW Himalaya, India. *Palaeogeogr. Palaeoclimatol. Palaeoecol.* 212, 95–118.
- Sangode, S.R., Phartiyal, B., Chauhan, O.S., Mazari, R.K., Bagati, T.N., Suresh, N., Mishra, S., Kumar, R., Bhattacharjee, P., 2007. Environmental magnetic studies on some Quaternary sediments of varied depositional settings in the Indian sub-continent. *Quatern. Int.* 159, 102–118.
- Sanyal, P., Sarkar, A., Bhattacharya, S.K., Kumar, R., Ghosh, S.K., Agrawal, S., 2010. Intensification of monsoon, microclimate and asynchronous C4 appearance: isotopic evidence from the Indian Siwalik sediments. *Palaeogeogr. Palaeoclimatol. Palaeoecol.* 296, 165–173.
- Singh, V., Tandon, S.K., 2010. Integrated analysis of structures and landforms of an intermontane longitudinal valley (Pinjaur dun) and its associated mountain fronts in the NW Himalaya. *Geomorphology* 114, 573–589.
- Suresh, N., Ghosh, S.K., Kumar, R., Sangode, S.J., 2004. Clay-mineral distribution pattern in Late Neogene fluvial sediments of the Subathu sub-basin, central sector of Himalayan foreland basin: implications for provenance and climate. *Sediment. Geol.* 163, 265–278.
- Tarling, D.H., 1983. *Paleomagnetism, Principles and applications in geology, geophysics and archaeology.* Chapman & Hall, New York, 379 p.
- Tauxe, L., Mullender, T.A.T., Pick, T., 1996. Potbellies, wasp-waisted, and superparamagnetism in magnetic hysteresis. *J. Geophys. Res.* 101 (B1), 571–583.
- Thomas, J.V., Parkash, B., Mohindra, R., 2002. Lithofacies and palaeosol analysis of the Middle and Upper Siwalik Groups (Plio–Pleistocene), Haripur–Kolar section, Himachal Pradesh, India. *Sediment. Geol.* 150, 343–366.
- Thompson, R., Oldfield, M., 1986. *Environmental magnetism.* Allen and Unwin, London, 227 p.
- Tripathi, C., 1986. Siwaliks of the Indian Subcontinent. *J. Palaeontol. Soc. India* 31, 1–8.
- Wasilewski, P., 1973. Magnetic hysteresis in natural materials. *Earth Planet. Sci. Lett.* 20, 67–72.